Article

Not peer-reviewed version

Thermal Stability and Purity of Graphene and Carbon Nanotubes: Key Parameters for Their Thermogravimetric Analysis (TGA)

Markus Martincic , Stefania Sandoval , Judith Oró , Gerard Tobías-Rossell *

Posted Date: 5 June 2024

doi: 10.20944/preprints202406.0317.v1

Keywords: carbon nanotubes; thermogravimetric analysis; purification; catalyst content

 doi:10.20944/preprints202406.0317.v1

Article

Thermal Stability and Purity of Graphene and Carbon Nanotubes: Key Parameters for Their Thermogravimetric Analysis (TGA)

Markus Martincic, Stefania Sandoval, Judith Oró-Solé and Gerard Tobías-Rossell *

Institut de Ciencia de Materiales de Barcelona (ICMAB-CSIC, Campus de la UAB, 08193 Bellaterra, Barcelona, Spain; markus.martincic@gmail.com (M.M.); ssandoval@icmab.es (S.S.); oro@icmab.es (J.O.-S.)

* Correspondence: gerard.tobias@icmab.es; Tel.: +34-935-801-853

Abstract: Thermal analysis is widely employed for the characterization of nanomaterials. It encompasses a variety of techniques that allow the evaluation of the physicochemical properties of a material by monitoring its response under controlled temperature. In the case of carbon nanomaterials, such as carbon nanotubes and graphene derivatives, thermogravimetric analysis (TGA) is particularly useful to determine the quality and stability of the sample, presence of impurities and the degree of functionalization or doping after post-synthesis treatments. Furthermore, TGA is widely used to evaluate the thermal stability against oxidation by air, which can be for instance enhanced by the purification of the material and by nitrogen doping, finding application in areas where a retarded combustion of the material is required. Herein, we have evaluated key parameters that play a role in the data obtained from TGA. Within this study we show that the thermogravimetric curve of carbon nanomaterials is greatly influenced by these parameters. This is important in terms of data recording and their analysis, since a poor control of the conditions of measurement might lead to false conclusions. We highlight this by analyzing different samples of graphene and carbon nanotubes where both thermal stability and sample purity assessment are found to be dependent on the employed TGA parameters. Finally, a set of TGA parameters are recommended for the analysis of carbon nanomaterials to obtain reliable data.¡

Keywords: carbon nanotubes; thermogravimetric analysis; purification; catalyst content

1. Introduction

Synthetic carbon allotropes, including both carbon nanotubes (CNTs) and graphene based systems, are regarded as a robust and versatile class of materials. They were brought to the attention of the scientific community by the discovery of the multi-walled and single-walled carbon nanotubes by Iijima in 1991[1] and 1993[2] respectively, and the first isolation and measurement of the graphene properties by Novoselov and Geim (leading to the conferring of the Novel Prize) in 2004.[3]

Carbon nanomaterials can be prepared using a variety of synthetic techniques that include arc discharge, laser ablation, chemical vapor deposition (CVD) and exfoliation of graphite. Particularly, when CVD is employed to obtain SWCNTs, the process usually leads to the formation of impurities such as amorphous carbon and metal (catalyst residue) and graphitic nanoparticles (that can also coat the catalyst particles) or fullerenes.[4] Since the presence of these species can interfere with the properties and quality of the tubular nanostructures, their removal using a purification step prior to their processing is usually required. When it comes to graphene, both CVD and exfoliation of graphite remain as the most commonly employed approaches. Modification of the electronic structure and intrinsic properties of graphene-based materials is usually obtained via the introduction of structural defects,[5,6] attaching inorganic and organic species via decoration and functionalization,[7–9] and doping.[10–12] Meanwhile, several strategies have been reported to potentiate, modify or take advantage of the characteristics of CNTs. They can be either endohedrally modified by introducing a variety of compounds within their hollow structure,[13] or undergo exohedral modification, by inducing structural doping or attaching bearing functionalities onto their

 doi:10.20944/preprints202406.0317.v1

walls.[14,15] Physical and chemical modification of carbon nanomaterials thus leads to a variety of systems that find applications in fields that include catalysis,[16] electronics[17] or biomedicine.[18]

One particular and relatively straightforward strategy to tune the properties of both graphene based materials and CNTs consists on the introduction of foreign atoms (chemical doping) within the honeycomb lattice that is the structural basis of both the 2D layers and the nanotubes walls, respectively.[19] Nitrogen doping is the most commonly used approach for this purpose, with a myriad of reports describing synthetic methodologies to embed N atoms within the carbonaceous skeleton, thus modifying the properties of the materials.[20–22] In this field, although research on doping CNTs[23] is not scarce, most efforts have been focused on the structural modification of graphene-based materials, by tuning two key parameters ruling the properties of the N-doped systems, namely, the concentration and nature of the N-based moieties.[24,25] N-doping allows tuning not only the conductivity,[26] but also other physico-chemical properties including mechanical properties,[24,27] and thermal stability[28]. As a consequence, N-doped carbon materials find application in fields like catalysis, batteries, sensors[29], electronics [30] and dye absorption.

In order to build a wide and precise portrait of the structure, morphology, composition, dimensionality and morphology, carbon nanomaterials are usually evaluated using a variety of characterization techniques. These include electron microscopy, X-ray diffraction, X-ray photoelectron, ICP, UV-Vis, IR-Vis and Raman spectroscopies and thermal analysis, to name some. Thermogravimetric analysis (TGA) is a simple, but widely used, technique to characterize carbon derivatives.[31,32] TGA allows monitoring temperature-induced physical and chemical changes to materials. By analyzing weight variations of the sample (thermal events), it is possible to determine the temperature at which a reaction takes place, and can thus provide information on the thermal stability of a material. Moreover, thermal events might offer useful information to elucidate the composition of the material and to study phenomena such as phase transitions, absorption/desorption, chemisorption, oxidation, degradation or solid-gas reactions. The atmosphere used during the measurement plays a significant role in the information collected from the analysis.[33] When performing TGA on carbon-based systems under oxidizing gases (O_2 or air), usually, a pronounced weight loss, typically occurring above 400 °C (temperature largely dependent on the sample), corresponds to the oxidation of the carbon skeleton into carbon dioxide, while the resulting residue (if so) might consists of oxidized inorganic materials, such as catalyst or other compounds employed for their synthesis or post-synthesis treatments.[4,34] Meanwhile, a weight loss, occurring at lower temperature (that in some cases can even overlap with the main thermal event) is usually attributed to the elimination of labile groups, namely, water molecules or also to bearing functionalities attached to the surface of the analyzed systems.[35,36] When using inert gases to perform TGA (argon, helium and nitrogen – although nitrogen could be regarded as a source of N in some cases –), the weight loss corresponds to the removal of functional groups because combustion of the sp^2 skeleton does not occur in absence of an oxidizing ambient.[37] Other parameters, like gas flow, heating rates and mass of sample may induce variations in the TG curve and therefore, affect the interpretation of the data collected from TGA. Here, we provide insights on the role of these parameters, providing tools for the selection of the optimal conditions to design reliable experiments and exploit the benefits of thermal analysis for the characterization of carbon nanomaterials. It is worth noting that a clear and detailed description of the conditions employed for the measurements of the thermal properties of the samples allows minimizing errors when comparing analysis performed. Previous studies have been devoted to analyze the oxidation of CNTs[38] and to explore the role of the parameters stablished to perform thermal analysis[39,40], however, a detailed analysis of their influence on the study of CNTs and graphene-based materials has not been reported.

2. Materials and Methods

2.1. Chemicals

Single-walled carbon nanotubes (SWCNTs, CVD) were provided by Thomas Swan Co. Ltd. Graphite powder (<20 μm), $NaNO_3$ (≥99 %) and $KMnO_4$ (99 %) were supplied by Sigma-Aldrich,

 doi:10.20944/preprints202406.0317.v1

while H_2SO_4 (98 %), HCl (37%) were acquired from Panreac. H_2O_2 (35 %) was obtained from Acros Organics. NH_3 gas (99.99 %) and Ar (99.99 %) were provided from Carburos Metálicos.

2.2. Methods

Purification of SWCNTs: In order to remove side-product resulting from the synthesis of CNTs,[41–43] 200 mg of SWCNTs were ground using an agate mortar and pestle. Afterwards, the sample was placed inside an opened-ended silica tube and subsequently located in a tubular furnace. The system was subsequently purged and kept under Ar atmosphere. The material was then treated with steam during 4 h at 900 °C. After cooling down, the sample was dispersed in 200 mL of 6 M HCl, and treated overnight at 110 °C (under reflux) in order to remove the Fe catalyst used for the CNTs synthesis. Samples were subsequently filtered under vacuum, washed with distilled water until neutral pH, collected and dried overnight at 60 °C.

Preparation of N-doped Reduced graphene oxide (N-doped RGO): To obtain a precursor susceptible to be modified (ammonolysis reactions (N-doping)), graphene oxide (GO) was prepared by a modified Hummer´s method.[24] Briefly, concentrated H_2SO_4 (57.5 mL), $NaNO_3$ (1.25 g) and graphite powder (2.5 g) were slowly mixed and cooled down to 0 °C. 30 min later, 7.5 g of $KMnO_4$ were added, keeping the system below 20 °C. The mixture was then warmed to 35 °C and simultaneously stirred during 30 min and cooled to room temperature. Afterwards, 115 mL of water were added carefully, and the temperature of the system was fixed at 98 °C for 2 h (reflux). Finally, 500 mL of water and 2.5 mL of a 30 % H_2O_2 solution (2.5 mL) were added. The content was cooled, centrifuged and washed with distilled water until neutral pH was reached.

N-doped RGO was synthesized by annealing GO in the presence of pure NH_3 gas. For this purpose, the sample (100 mg) was placed inside a quartz tube located in a sandwich furnace and treated during 1 h with at the selected temperature with the gas flowing at a 300 mL min^{-1} rate.

2.3. Characterization

SWCNTs Samples were evaluated using a TA instrument TGA Q5000-IR working under a 10 mL min^{-1} balance flow of N2. In all cases, synthetic air (80:20 N2:O2) was used as oxidizing atmosphere. To evaluate the influence of the parameters of measurement in the combustion process, 1-20 mg of CNT were annealed under heating rates ranged between 1 °C min^{-1} and 50 °C min^{-1}. Meanwhile, the flow rates of air, ranged between 5 mL min^{-1} and 200 mL min^{-1}, were employed during TG analyses. The protocol involved locating the sample into a platinum pan, protected to prevent its fusion during the analysis.

The residue obtained after the annealing treatments was analyzed using Scanning Electron Microscopy (SEM). The morphology of the sample was evaluated using a QUANTA FEI 200 FEG-ESEM, while Energy Dispersive X-ray Spectroscopy (EDS) allowed to determine the elemental composition of the material. The Diffraction pattern of the crystals obtained after the combustion of the nanotubes was obtained from a 120 KV JEM1210 (JEOL) TEM. Samples for microscopy were prepared by sonicating a small amount of sample in pure ethanol. Afterwards, the obtained dispersion was placed dropwise onto a lacey copper grid.

3. Results and discussion

Due to their ease of manipulation, CNTs will be initially used to understand the role of the different TGA parameters. To complete the study, graphene-based materials will also be investigated.

Figure 1a) shows the thermogravimetric curve, resulting from plotting the % weight of as-received (raw) CNTs with respect to temperature. In this case the material is annealed under flowing air (25 mL min^{-1}, 10 °C min^{-1}) up to 900 °C. As it can be observed, a main thermal event occurs when annealing SWCNTs under an oxidizing atmosphere (air). The annealing treatment has induced the total combustion of the carbonaceous fraction, while a solid residue, probably resulting from the oxidation of the inorganic fraction has been obtained, and collected after cooling down.

 doi:10.20944/preprints202406.0317.v1

The TGA curve is a useful tool to analyze the oxidation process of a material. Four main temperatures can be defined to describe the process that occurs when the sample undergoes the oxidation; three of which can be determined directly from the resulting plot. T_{onset} and T_{offset} give a temperature range in where the oxidation takes place, while T_{50} corresponds to the temperature at which 50 % of weight loss occurs. An additional value, T_0, can be obtained from the derivative thermogravimetry (DTG) curve (dw/dT) and it is defined as the temperature of the maximum in the weight loss rate. Finally, from DTG we can also calculate the surface area underneath the peak, A. It is worth noting that a comparison between A values is not possible for treatments performed at different heating rates, because this area is also time dependent.

Additionally, in order to obtain a precise overview of the material, the composition of the residue remnant from the process was assessed. In this case, SEM along with EDS analysis was carried out (**Figure 1 b)**). The obtained spectrum revealed the presence of both iron and oxygen, probably corresponding to an iron oxide, resulting from the oxidation (during the TGA) of iron catalyst, already present in the sample from the synthesis process. The structure of the residue has been determined by electron diffraction.

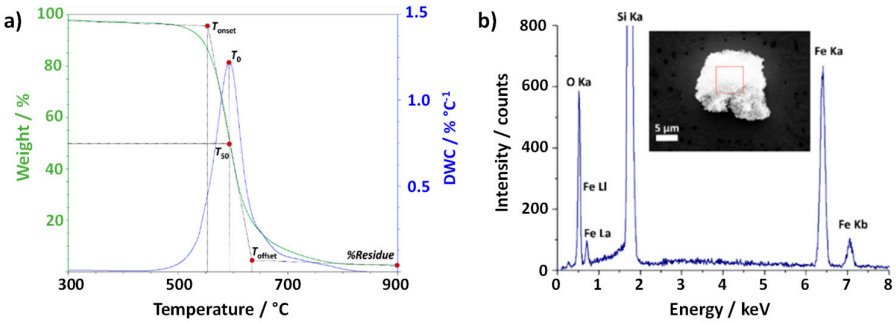

Figure 1. (**a**) TGA (green line) and DTG (blue line) resulting from annealing raw SWCNTs up to 900 °C, under are (flow rate 25 mL min^{-1}). (**b**) SEM micrograph (inset) and EDS resulting from analyzing a selected area (red square) of the residue collected after the annealing process. Fe and O signals are attributed to of iron oxide from the oxidation of iron used as catalyst for the growth of the SWCNTs.

Figure 2 shows the morphology of the collected residue by TEM, along with its selected area electron diffraction (SAED) pattern. In both, monocrystalline and polycrystalline areas, the patterns correspond to iron(III) oxide, hematite. Therefore, the presence of other iron derivatives (ex. iron carbide) or species, previously detected in CNTs can be discarded.[44]

TGA requires the definition of certain experimental parameters, such as sample mass, heating rate and glass flow. In order to determine their role in the resulting TGA data, several experiments were next performed. TGA was carried out on both raw and purified SWCNTs. In all cases, the sample was initially allowed to stabilize at rt for 20 min. Afterwards, it was heated up to 120 °C, at 10 °C min^{-1}. The system was isothermally kept during 20 minutes, under a constant air flow (20 mL min^{-1}). This step was performed to eliminate any water or volatile species, from the environment, that might have physisorbed onto the sample. Afterwards, the system was annealed up to 900 °C and then allowed to cool down to room temperature. For statistical purposes and to get reliable data, five replicas were performed for each experiment.

Initially, the influence that the employed sample mass has on the TGA curve was evaluated. Both flow rate (25 mL min^{-1}) and heating rate (10 °C min^{-1}) were kept invariable during the analysis. Figure 3a,b register both the thermogravimetric and the calculated derivative curves obtained after annealing 1, 2, 5, 10 and 20 mg of raw SWCNTs under air. Visual inspection of TGA curves suggests slight variations in terms of combustion temperatures when different amounts of material were employed. Let us initially focus on the temperatures at which the thermal events initiate (T_{onset}). No major differences in T_{onset} are observed when changing the mass of sample (from 1 to 20 mg; Figure 3c). In contrast, a more pronounced variation is perceived in the T_{offset} values. Whereas the T_{onset}

 doi:10.20944/preprints202406.0317.v1

remains barely constant in the range of 1-10 mg, a significant increase is clearly visible when using 15 mg and 20 mg of sample (reaching up to 650 °C and 681 °C, respectively). This suggests that, once the minimum temperature required for starting the oxidation is reached, the combustion of the sample already starts, but the more sample is present the longer time it takes to complete the oxidation process. This is reflected by a prolongation of the thermal event thus inducing variations in shape of the thermogravimetric curve.

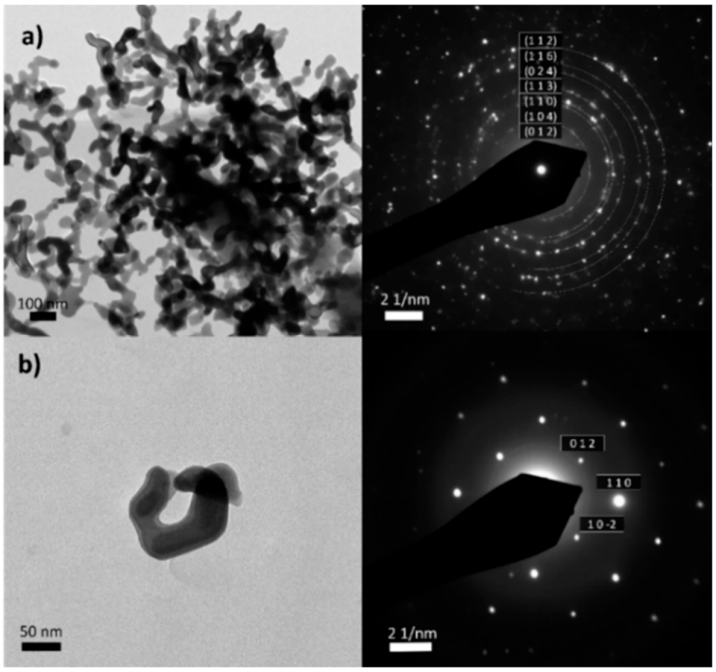

Figure 2. TEM and electron difraction analysis of the residue collected after the TGA of raw SWCNTs.

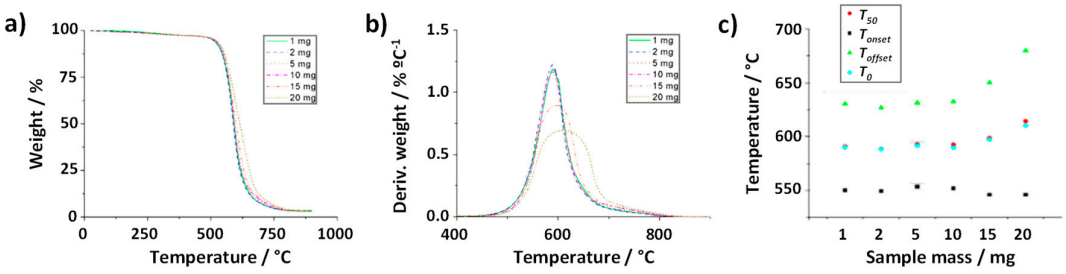

Figure 3. TGA of raw SWCNTs using different amounts of sample (1, 2, 5, 10, 15, 20 mg) up to 900 °C under synthetic air while keeping gas flow (25 mL min^{-1}) and heating rate (10 °C min^{-1}) constant. a) TGA, b) DTG, c) temperatures determined for T_{onset}, T_{offset}, T_0 and T_{50}.

As it was explained above, DTG curves resulting from calculating dw/dT (**Figure 3** b)) allow determining the temperature at which the weight loss rate reaches its maximum (T_0, solid blue circles). However, further information can be obtained by the analysis of the DTG curve, with respect to the quality, morphologic characteristics or heterogeneity of the sample. For instance, the width of the DTG curve can be used as an indicator of material purity, where a narrower peak might correspond to the presence of a higher purity material. It is also possible to discern between two or more overlapping reactions. In our study, the difference in the shape of the curves cannot be attributed to sample heterogeneity because all the analyses were carried out using the same batch of

 doi:10.20944/preprints202406.0317.v1

CNTs. Therefore, it only depends on the time elapsed between the start of the thermal event and the complete combustion of the sample.

The presence of inorganic impurities, in the present case iron catalyst, can also be determined by TGA taking into account the residual weight after the complete oxidation of the sample, which as observed by ED corresponds to Fe_2O_3. Therefore, it is possible to quantitatively determine the iron present in the sample by simple stoichiometry (Figure 4a). Similar values are obtained within experimental error (error bar included for one of the analysis) regardless of the employed mass. Nevertheless, a lower small of iron content would seem to be present when using only 1 mg of sample. Therefore, using larger amounts of sample, whenever possible, would be desirable.

Next, the role of the gas flow rate was assessed. To minimize the experimental error that might be induced by using a low amount of sample, 5 mg of SWCNTs were employed. TGA were performed by annealing raw SWCNTs at a heating rate of 10 °C min^{-1} up to 900 °C, under flowing air at 5, 10, 25, 50, 100, 150 and 200 mL min^{-1}. As it can be observed in Figure 4b significant differences are observed after calculating the amount of iron catalyst present in raw SWCNTs from the different TGA curves. There is a clear tendency to determine a much larger amount of catalyst content when using the highest flow rates (150 and 200 mL min^{-1}). The use of a large flow rate may induce a slight push up of the platinum pan employed for the analysis thus altering the TGA output data. Therefore, the use of flow such high flow rates does not seem appropriate to study this type of materials.

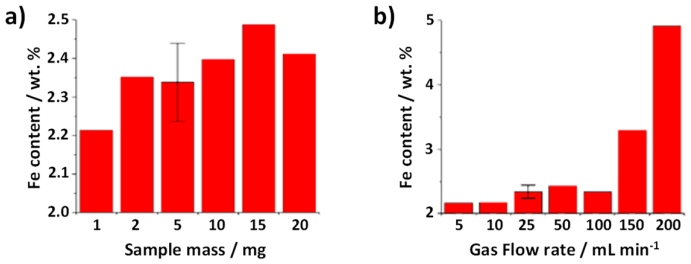

Figure 4. a) Iron catalyst content calculated from the collected residue after TGA of raw SWCNTs. The catalyst content was determined taking into account that a complete oxidation to iron(III) oxide occurs during the TGA.

Figure 5a,b shows the thermogravimetric curves resulting from the above-mentioned treatments, along with their DTG curves. Similarly to the previous case, the variation in the T_{onset} for the range of gas flow rates investigated does not show significant differences, suggesting that this parameter does not play a significant role in the start of the oxidation. However, a delay in the complete oxidation of the sample (T_{offset}) is clearly visible when using low gas flow rates, namely 5 mL min^{-1} (continuous green line) and 10 mL min^{-1} (blue dotted line). This might be induced by the lack of oxygen supply, which is crucial for the combustion of the tubular carbon nanostructures. The longer lapse of time required to finish the thermal event, makes the T_{offset} values shift towards significantly higher temperatures for the samples treated under lower flow rates (691°C and 656 °C, for 5 mL min^{-1} and 10 mL min^{-1}, respectively), as it can be appreciated in Figure 5c. As expected, wider DTG peaks can be observed from the 5 and 10 mL min^{-1} analyses (Figure 5b). In the case of the TGA at 5 mL min^{-1} a T_0 of more than 30 °C is observed with respect to TGA performed at ≥ 25 mL min^{-1}.

Finally, the role played by the heating rate in the oxidation process was evaluated. For this purpose, a series of annealing treatments were performed on 5 mg of CNTs using an air flow rate of 25 mL min^{-1}. The heating rates employed were 1, 5, 10, 15, 20 and 50 °C min^{-1}. The resulting TGA are shown in Figure 6a. As it can be observed, this parameters turned out to play the major role and important changes can be observed, both in terms of the shape of the TGA curve and temperatures at the oxidation occurs. Visual inspection suggests that there is a direct relationship between the heating rate and the temperature of combustion of the CNTs, with a range of T_{onset} between 483 °C and 582 °C. Moreover, TG curves of the samples treated under both the lower (1 °C min^{-1}) and the higher temperature (50 °C min^{-1}) rates are clearly differentiated from those annealed under

 doi:10.20944/preprints202406.0317.v1

temperature rates ranged between 5 and 20 °C min^{-1}. It is worth noting though that the catalyst content determined under the different heating rates was similar within experimental error (Figure 6c). According to previous reports, thermal conductivity and transition kinetics might affect more significantly when the heating rate is modified. Instrument effects may also play a role.[45,46] In case of the evaluated nanocarbons, one additional aspect should be considered. As mentioned before, the presence of impurities, resulting from the CVD process, alters the characteristics of the sample. For instance, the oxidation of amorphous carbon is known to occur at lower temperatures than CNTs.[47] The presence of this impurity in the raw material could account for the early combustion observed when the sample is treated a 1 °C min^{-1} (continuous green line). Once the combustion of the amorphous carbon starts to take place, the temperature of the system might locally increase because it is an exothermic process (releases energy), which might in turn result into the earlier oxidation of the nanotubes. This phenomenon becomes more visible when using the slowest heating rate. Despite a continuous increase of T_{onset} is observed when increasing the heating rate, the width of the thermals event remains almost invariable up to 20 °C min^{-1} (T_{offset}-T_{onset} ~ 78 °C, Figure 6d), with symmetric DTG curves Figure 6b that suggest negligible during the oxidation process once started.

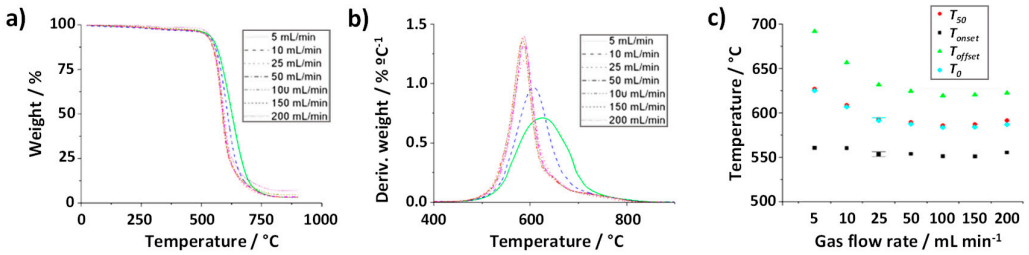

Figure 5. TGA of raw SWCNTs using different flow rates (5, 10, 25, 50, 100, 150, 200 mL min^{-1}) up to 900 °C under synthetic air while keeping the mass of sample (5 mg) and heating rate (10 °C min^{-1}) constant. a) TGA, b) DTG, c) temperatures determined for T_{onset}, T_{offset}, T_0 and T_{50}.

Interestingly, at the highest flow rate (50 °C min^{-1}) marked differences in the shape of the TGA curve are appreciated, which result in a large broadening of the DTG curve (T_{offset}-T_{onset} ~182 °C, **Figure 6d**). It is worth noticing that at the end of the TGA at 900 ºC the collected residue was black, indicating that the carbon fraction had not been completely oxidized, and it was necessary, only in this case, to perform the analysis up to 1000 ºC to achieve a complete oxidation of the sample.

The capability of the thermobalance to homogeneously heat the sample can contribute to the obtained results. Let us consider that the temperature of the furnace increases from A to B. In order to obtain appropriate and trustable data of the process, the entire sample might reach the target conditions (temperature B), homogeneously, before its weight is registered by the equipment; on the contrary, the analysis might induce to deviations between the temperature of the program and the real temperature (T_{real}) of the sample.This is the case when the system is annealed too fast and T_{real} is lower than the expected temperature (T set in the controller). This is the case of the sample analyzed at a heating rate of 50 °C min^{-1}. The slope of the TG curve also decreases due to a more prolonged time of oxidation of the sample (T_{offset} ~764 °C), similarly affecting the calculation of the DTG.

By analyzing the set of parameters above described we have clearly stressed the importance, not only of carefully selecting the conditions of the measurements in TGA, but also of using always the same parameters, to obtain suitable and comparable information from this technique. Next, to complete the study we will analyze thermal curves resulting from the oxidation of as-received (raw) and purified SWCNTs. Initially, and according to the results obtained above, we employed the following parameters to obtain reliable information from the analysis: 5 mg of sample, a heating rate of 10 °C min^{-1} and a gas flow of 25 mL min^{-1}. These parameters were selected considering aspects like the shape of the TG curve (which indicates the homogeneity of the oxidation process), variations in the commencement and completion of the thermal event, and determination of the inorganic residue. Figure 7a shows both TGA and DTG curves of the analyzed materials. Purified SWCNTs

 doi:10.20944/preprints202406.0317.v1

were obtained performed using a previously reported steam and acid treatment,[49] which allows the efficient removal of amorphous carbon, graphitic particles and metal catalyst from the sample. The removal of these impurities results in a higher thermal stability of the sample, thus requiring higher energy to undergo the combustion, compared to the pristine one. This is in agreement with the shift of T_0 (DTG curve) for the purified CNTs with respect to the raw material.

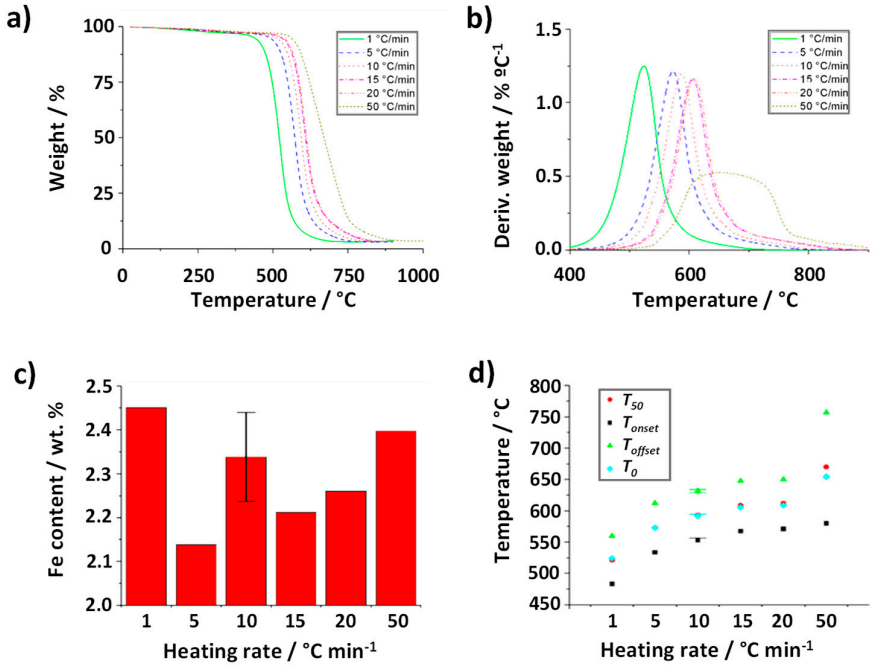

Figure 6. TGA of raw SWCNTs using different heating rates (1, 5, 10, 15, 20, 50 °C min^{-1}) up to 900 °C under synthetic air while keeping gas flow (25 mL min^{-1}) and sample mass (5 mg) constant. a) TGA, b) DTG, c) Temperatures determined for T_{onset}, T_{offset}, T_0 and T_{50}.

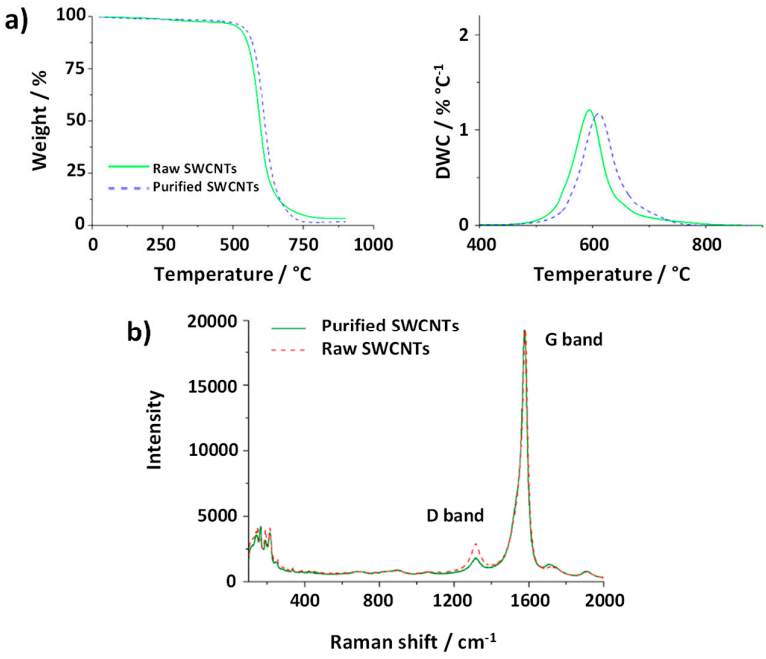

Figure 7. TGA and DTG of purified and raw SWCNTs, using 5 mg of sample, a heating rate of 10 °C min^{-1} and an air gas flow of 25 mL min^{-1}. b) Raman spectra of raw and purified SWCNTs.

 doi:10.20944/preprints202406.0317.v1

Raman spectroscopy provides information about the structure, crystallinity and purity of the CNTs. Two bands are commonly present in the CNTs Raman spectra. The first one, located around 1570 cm^{-1} corresponds to the E_2g photon at the Brillouin zone center and it is characteristic of the vibrations of sp^2 C atoms along the graphitic conjugated network. Meanwhile, the D band (around 1350 cm^{-1}) results from stimulating sp^3 carbon atoms, being generally attributed to the presence of defects in the structure of the CNTs. Moreover, these vibrations would also be associated to the presence of non-crystalline structures in the sample, as in the case of amorphous carbon. Thus, the I_D/I_G ratio is, usually employed as an indicator of the quality of the CNTs. Raman spectra of both purified and raw CNTs are shown in Figure 7b. The spectra were normalized for comparison. After the purification treatment the D band decreased (I_D/I_G ratio from 13.7 ± 0.4 to 9.8 ± 1.6 (N=4)). Since the purification protocol involves annealing the material under a mixture of steam/argon at 900 °C, the increase in the crystallinity of the sample can be attributed either to the elimination of defects of the CNTs walls or to the removal of amorphous carbon. Therefore, Raman spectroscopy provides evidence on the indirect information extracted from TGA. SQUID was also performed for monitoring the content of catalyst in the samples. In agreement with TGA, the amount of Fe after purification decreased, starting from 1.4 wt. % (3.1 emu/g) for the raw material, down to 0.5 wt. % of Fe (1.1 emu/g) for the purified CNTs. Finally, elemental analysis revealed an increase in the C content after the purification (from 91.4% for raw material to 96.9% after purification), as consequence of the removal of metal catalyst by the acid treatment.

These to samples where then employed to illustrate the effect of the previsouly discussed TGA parameters on the resulting curves. First, the amount of sample was changed. Figure 8a shows the TGA and DTG curves resulting from the analysis of 1 mg of purified SWCNTs and 20 mg of the raw material (25 mL min^{-1} gas flow and heating rate of 10 °C min^{-1}). Comparision of the data with the TGA curves obtained using the same TGA parameters for both samples (Figure 7a), reveals that the increase in the amount of raw nanotubes results in a delay in the T_{offset}. This is probably because the presence of a large amount of sample requires either more energy or time for the total combustion under similar conditions. As consequence, the determination of the thermal stability of the materials can be compromised when using different amounts of samples, as in the case of Figure 8a, where raw SWCNTs would seem to present a higher thermal stability than the purified SWCNTs, thus leading to false conclusions.

An inverse effect is observed when comparing samples treated under different heating rates Figure 8b. If the TGA curve of purified CNTs annealed at 10 °C min^{-1} is compared with the TGA of raw material oxidized at 50 °C min^{-1} (sample mass 5 mg, gas flow 25 mL min^{-1}) the slope of the TG curve varies, being more pronounced for the purified sample. When using a higher flow rate for purified CNTs (200 mL min^{-1}) than for raw CNTs (25 mL min^{-1}) to anneal 5 mg of sample at a heating rate of 10 °C min^{-1} (Figure 8c), the relative residue of the raw sample seems to increase, leading to an Fe content of 3.1 wt. %, which is markedly superior to the Fe calculated from the curve obtained from the experiment performed on pristine CNTs at lower flow rate (2.3 wt. %, Figure 7a). The observed inversed quantity of catalyst among raw and purified SWCNTs would also result in false conclusions, because the amount of iron is decreased by purification, as determikned by SQUID.

 doi:10.20944/preprints202406.0317.v1

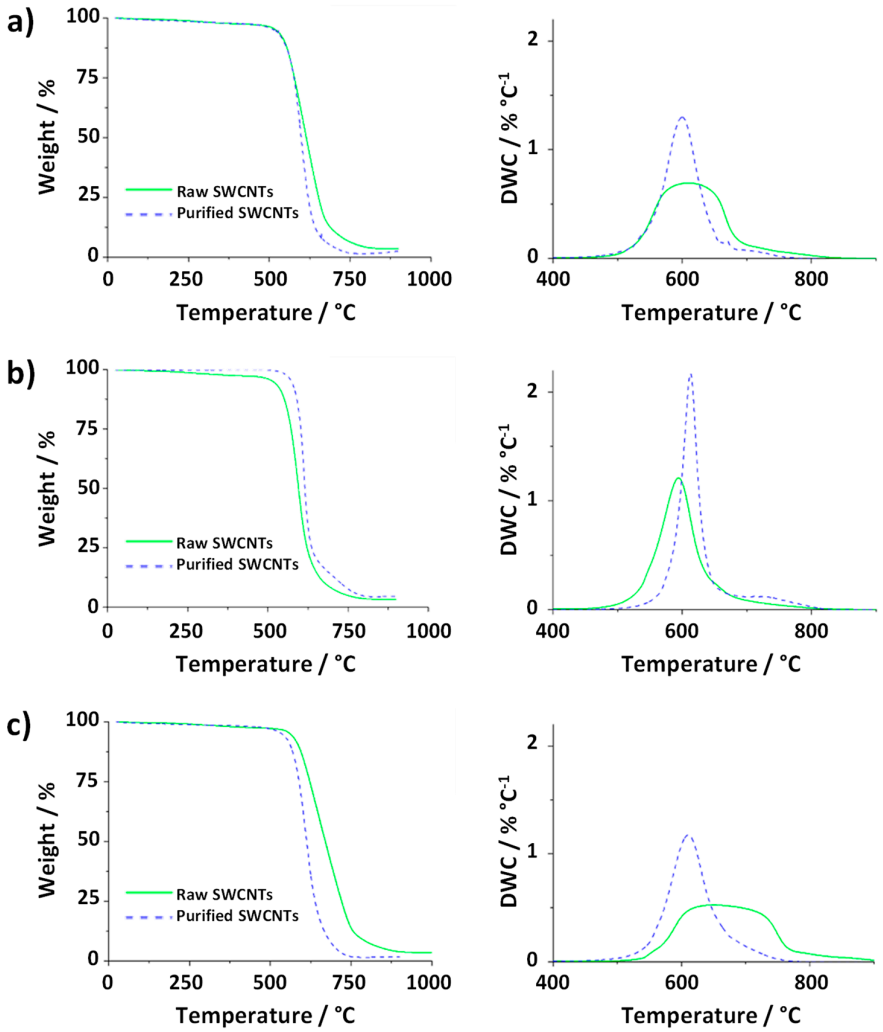

Figure 8. TGA and DTG of the same purified and raw SWCNTs. a) purified (1 mg) and raw (20 mg) with a heating rate of 10 °C min^{-1} and an air gas flow of 25 mL min^{-1}, b) TGA heating rate of 10 °C min^{-1} (purified) and 50 °C min^{-1} (raw) with 5 mg and an air gas flow of 25 mL min^{-1}, c) TGA gas flow of 200 mL min^{-1} (purified) and 25 mL min^{-1} (raw) using 5 mg of sample and a heating rate of 10 °C min^{-1}.

One particular case, in which the determination of the thermal stability by TGA is especially useful, includes the evaluation of carbon nanomaterials which structure have been modified via covalent or not covalent functionalization. A variety of reports have demonstrated that, for instance, the introduction of foreign species within the sp^2 skeleton via replacing C atoms by dopant species like boron or nitrogen, not only induces changes in the electronic behavior of the material, but also affects the stability of the sample and its response against physical and chemical processes like thermal transport[50] or oxidation.[51][52] In order to have insights about the role of the TGA conditions in the evaluation of modified planar nanocarbons, we have analyzed a material that we previously reported, which has demonstrated an enhanced thermal stability against the oxidation by air compared with its non-doped counterpart.[53] The sample (N-doped reduced graphene oxide, hereafter N-doped RGO) resulted from the ammonolysis treatment of graphene oxide (GO) using pure ammonia gas at 500 °C for 1 h. By performing TGA of the sample (2 mg, heating rate 10 °C min^{-1}) along with other characterization techniques, we have demonstrated that the introduction of N atoms within the honeycomb lattice of graphene induced up to 162 °C increase in the T_{onset} with respect to a sample prepared under the same experimental conditions but replacing ammonia by argon. As shown in Figure 9a an important difference between T_{onset} of the samples is observed in the TGA curves of both RGO and N-doped RGO, performed under the same TGA parameters. Next, we

 doi:10.20944/preprints202406.0317.v1

analyzed the samples using markedly different conditions. Figure 9b shows the TGA curves of RGO treated at the highest heating rate employed in this work, 50 °C min^{-1}, while N-doped RGO was annealed using a heating rate much more low, 0.2 °C min^{-1}. Such a low heating rate, not previously employed within this work, was used with the aim to obtain marked differences between the analyses. Both, sample weight and air flow were kept constant. Due to the long duration of the treatment performed to the N-doped sample, and considering that no thermal event would occur under 300 °C, an initial heating rate of 10 °C min^{-1} was employed up 300 °C, to reduce the total time of analysis. Then the system was annealed at 0.2 °C min^{-1} until the sample underwent its total combustion. The sudden change in the heating rate results in an apparent increase of the sample weight. This can be considered an artifact of the measurement, likely due to the lengthy measurement, of almost one day and a half (Figure 9e represents the weight % vs time for N-doped RGO; Figure 9d for RGO). Despite the weight % is no longer relevant and also a high residual value is obtained, the temperature at which the oxidation process takes place it is worth discussion. In case of both reduced GO and N-doped RGO, the temperature at which the combustion takes place agrees with the behavior of the evaluated SWCNTs. A significant increase of the heating rate (from 10 °C min^{-1} to 50 °C min^{-1}) induces a shift of T_{offset} towards higher T (from 475 °C to 502 °C for the annealed RGOs). In case of the N-doped RGO, the use of a very slow heating rate results in a dramatic reduction of the T_{offset}, from 599 °C to 462 °C. In this way, both samples N-doped RGO and RGO, would seem to have the same thermal stability against oxidation. The use of a slow heating rate, for N-doped RGO, results in a narrower DTG curve than RGO.

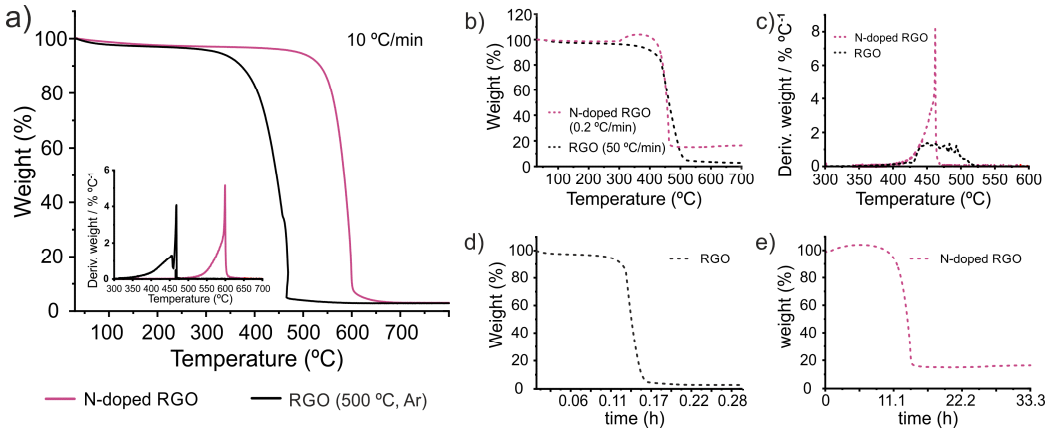

Figure 9. TGA curves resulting from annealing 2 mg of a) RGO (continuous black line) and N-doped RGO (continuous red line) at a heating rate of 10 °C min^{-1} (the DGT curves are showed in the inset), b) RGO at 50 °C min^{-1} (dotted black line) and N-doped RGO at 0.2 °C min^{-1} (dotted red line). c) The DTG curves calculated from TG curves registered in b). e) TG curves (from treatments in b)) plotted vs the time of treatment. All the samples were heated under a constant flow of air.

4. Conclusions

The proper physical and chemical characterization of carbon nanomaterials, which include carbon nanotubes and graphene derivatives, plays a crucial role to exploit their unique properties. Evaluating aspects like thermal and chemical stability, or the analysis of the response of the materials against external stimuli, provide insights about their potential applications.

TGA provides valuable information for the evaluation of these materials, as in case of the thermal stability of N-doped graphene derivatives, included here. However, several parameters must be controlled in order to obtain reliable information from measurements. We have evaluated aspects like amount of sample, heating rate and gas flow rate, used when TGA is performed and their effect in the combustion process of both carbon nanotubes and graphene derivatives.

In case of the CNTs used here, we found out that, the modification of the heating rate played the major role in the process of combustion in presence of air, leading to significant variations in the

 doi:10.20944/preprints202406.0317.v1

temperature at which the oxidation starts to occur (from 483 to 582 °C), affecting the duration of the processes (with differences of T_{offset} up to 200 °C when using the lowest and the highest heating rate), or even leading to different amounts of residue after the annealing treatment ended.

Taking into account the data collected from this study, we propose the use of 2 to 10 mg of sample, a gas flow rate in the range of 25 and 100 mL min^{-1} and a heating rate of 10 °C min^{-1} for the TGA of carbon nanomaterials. Nevertheless, it is worth pointing out that these might need to be adjusted depending on the TGA equipment employed, because for instance the configuration of some equipments allows the analysis of larger amounts of samples.

We believe that this study, which has allowed to stablish suitable conditions to perform the TGA, might also be considered for the characterization of other inorganic, organic or composite materials.

Author Contributions: Conceptualization, M.M., G.T.-R.; methodology, M.M., J.O.-S., S.S.; investigation, M.M., J.O.-S., S.S.; writing—original draft preparation, M.M., SS; writing—review and editing, J.O.-S., S.S., G.T.-R.; supervision, G.T.-R.; funding acquisition, G.T.-R. All authors have read and agreed to the published version of the manuscript.

Funding: This work was supported by the ERC Consolidator Grant NEST and the State Investigation Agency, through PID2020-113805 GB-I00 and the Severo Ochoa Programme for Centres of Excellence in R&D (CEX2023-001263-S),

Acknowledgments: The authors would like to thank Thomas Swan Co. Ltd. for providing carbon nanotube material used for this study.

Conflicts of Interest: The authors declare no conflict of interest.

References

1. Iijima, S. Helical Microtubules of Graphitic Carbon. *Nature* **1991**, *354*, 56–58, doi:10.1038/354056a0.
2. Iijima, S.; Ichihashi, T. Single-Shell Carbon Nanotubes of 1-Nm Diameter. *Nature* **1993**, *363*, 603–605, doi:10.1038/363603a0.
3. Novoselov, K.S.; Geim, A.K.; Morozov, S. V; Jiang, D.; Zhang, Y.; Dubonos, S. V; Grigorieva, I. V; Firsov, A.A. Electric Field Effect in Atomically Thin Carbon Films. *Science (1979)* **2004**, *306*, 666–669, doi:10.1126/science.1102896.
4. Hou, P.-X.; Liu, C.; Cheng, H.-M. Purification of Carbon Nanotubes. *Carbon N Y* **2008**, *46*, 2003–2025, doi:https://doi.org/10.1016/j.carbon.2008.09.009.
5. Banhart, F.; Kotakoski, J.; Krasheninnikov, A. V Structural Defects in Graphene. *ACS Nano* **2011**, *5*, 26–41, doi:10.1021/nn102598m.
6. Zhang, X.; Chen, H.; Qiao, D.; Yang, M. Effects of Structure Defects on Thermal Transport at the Graphene–Water Interface. *Adv Mater Interfaces* **2023**, *10*, 2202518, doi:https://doi.org/10.1002/admi.202202518.
7. Ferrer-Ugalde, A.; Sandoval, S.; Pulagam, K.R.; Muñoz-Juan, A.; Laromaine, A.; Llop, J.; Tobias, G.; Núñez, R. Radiolabeled Cobaltabis(Dicarbollide) Anion–Graphene Oxide Nanocomposites for In Vivo Bioimaging and Boron Delivery. *ACS Appl Nano Mater* **2021**, *4*, 1613–1625, doi:10.1021/acsanm.0c03079.
8. Guo, Z.; Chakraborty, S.; Monikh, F.A.; Varsou, D.-D.; Chetwynd, A.J.; Afantitis, A.; Lynch, I.; Zhang, P. Surface Functionalization of Graphene-Based Materials: Biological Behavior, Toxicology, and Safe-By-Design Aspects. *Adv Biol* **2021**, *5*, 2100637, doi:https://doi.org/10.1002/adbi.202100637.
9. Xiao, Y.; Pang, Y.X.; Yan, Y.; Qian, P.; Zhao, H.; Manickam, S.; Wu, T.; Pang, C.H. Synthesis and Functionalization of Graphene Materials for Biomedical Applications: Recent Advances, Challenges, and Perspectives. *Advanced Science* **2023**, *10*, 2205292, doi:https://doi.org/10.1002/advs.202205292.
10. Liu, H.; Liu, Y.; Zhu, D. Chemical Doping of Graphene. *J Mater Chem* **2011**, *21*, 3335–3345, doi:10.1039/C0JM02922J.
11. Singh, A.K.; Singh, R.S.; Singh, A.K. Recent Developments in Chemical Doping of Graphene Using Experimental Approaches and Its Applications. *Adv Eng Mater* **2022**, *24*, 2200259, doi:https://doi.org/10.1002/adem.202200259.
12. He, H.; Kim, K.H.; Danilov, A.; Montemurro, D.; Yu, L.; Park, Y.W.; Lombardi, F.; Bauch, T.; Moth-Poulsen, K.; Iakimov, T.; et al. Uniform Doping of Graphene Close to the Dirac Point by Polymer-Assisted Assembly of Molecular Dopants. *Nat Commun* **2018**, *9*, 3956, doi:10.1038/s41467-018-06352-5.

13. Poudel, Y.R.; Li, W. Synthesis, Properties, and Applications of Carbon Nanotubes Filled with Foreign Materials: A Review. *Materials Today Physics* **2018**, *7*, 7–34, doi:https://doi.org/10.1016/j.mtphys.2018.10.002.
14. Georgakilas, V.; Gournis, D.; Tzitzios, V.; Pasquato, L.; Guldi, D.M.; Prato, M. Decorating Carbon Nanotubes with Metal or Semiconductor Nanoparticles. *J Mater Chem* **2007**, *17*, 2679–2694, doi:10.1039/B700857K.
15. Dubey, R.; Dutta, D.; Sarkar, A.; Chattopadhyay, P. Functionalized Carbon Nanotubes: Synthesis, Properties and Applications in Water Purification, Drug Delivery, and Material and Biomedical Sciences. *Nanoscale Adv* **2021**, *3*, 5722–5744, doi:10.1039/D1NA00293G.
16. Kadam, S.A.; Sandoval, S.; Bastl, Z.; Simkovičová, K.; Kvítek, L.; Jašík, J.; Olszówka, J.E.; Valtera, S.; Vaidulych, M.; Morávková, J.; et al. Cyclohexane Oxidative Dehydrogenation on Graphene-Oxide-Supported Cobalt Ferrite Nanohybrids: Effect of Dynamic Nature of Active Sites on Reaction Selectivity. *ACS Catal* **2023**, *13*, 13484–13505, doi:10.1021/acscatal.3c02592.
17. Rho, Y.; Lee, K.; Wang, L.; Ko, C.; Chen, Y.; Ci, P.; Pei, J.; Zettl, A.; Wu, J.; Grigoropoulos, C.P. A Laser-Assisted Chlorination Process for Reversible Writing of Doping Patterns in Graphene. *Nat Electron* **2022**, *5*, 505–510, doi:10.1038/s41928-022-00801-2.
18. Wang, J.T.-W.; Klippstein, R.; Martincic, M.; Pach, E.; Feldman, R.; Šefl, M.; Michel, Y.; Asker, D.; Sosabowski, J.K.; Kalbac, M.; et al. Neutron Activated 153Sm Sealed in Carbon Nanocapsules for in Vivo Imaging and Tumor Radiotherapy. *ACS Nano* **2020**, *14*, 129–141, doi:10.1021/acsnano.9b04898.
19. Boshir Ahmed, M.; Alom, J.; Hasan, Md.S.; Asaduzzaman, Md.; Rahman, Md.S.; Hossen, R.; Abu Hasan Johir, M.; Taufiq Alam, M.; Zhou, J.L.; Zhu, Y.; et al. General Doping Chemistry of Carbon Materials. *ChemNanoMat* **2023**, *9*, e202200482, doi:https://doi.org/10.1002/cnma.202200482.
20. Wei, Q.; Tong, X.; Zhang, G.; Qiao, J.; Gong, Q.; Sun, S. Nitrogen-Doped Carbon Nanotube and Graphene Materials for Oxygen Reduction Reactions. *Catalysts* 2015, *5*, 1574–1602.
21. Lim, S.H.; Elim, H.I.; Gao, X.Y.; Wee, A.T.S.; Ji, W.; Lee, J.Y.; Lin, J. Electronic and Optical Properties of Nitrogen-Doped Multiwalled Carbon Nanotubes. *Phys Rev B* **2006**, *73*, 45402, doi:10.1103/PhysRevB.73.045402.
22. Lee, W.J.; Maiti, U.N.; Lee, J.M.; Lim, J.; Han, T.H.; Kim, S.O. Nitrogen-Doped Carbon Nanotubes and Graphene Composite Structures for Energy and Catalytic Applications. *Chemical Communications* **2014**, *50*, 6818–6830, doi:10.1039/C4CC00146J.
23. Ayala, P.; Arenal, R.; Rümmeli, M.; Rubio, A.; Pichler, T. The Doping of Carbon Nanotubes with Nitrogen and Their Potential Applications. *Carbon N Y* **2010**, *48*, 575–586, doi:https://doi.org/10.1016/j.carbon.2009.10.009.
24. Sandoval, S.; Kumar, N.; Oro-Solé, J.; Sundaresan, A.; Rao, C.N.R.; Fuertes, A.; Tobias, G. Tuning the Nature of Nitrogen Atoms in N-Containing Reduced Graphene Oxide. *Carbon N Y* **2016**, *96*, 594–602, doi:https://doi.org/10.1016/j.carbon.2015.09.085.
25. Sandoval, S.; Tobias, G. Tuning the Nature of N-Based Groups From N-Containing Reduced Graphene Oxide: Enhanced Thermal Stability Using Post-Synthesis Treatments. *Nanomaterials* 2020, *10*.
26. Podyacheva, O.Yu.; Ismagilov, Z.R. Nitrogen-Doped Carbon Nanomaterials: To the Mechanism of Growth, Electrical Conductivity and Application in Catalysis. *Catal Today* **2015**, *249*, 12–22, doi:https://doi.org/10.1016/j.cattod.2014.10.033.
27. Pinto, S.C.; Gonçalves, G.; Sandoval, S.; López-Periago, A.M.; Borras, A.; Domingo, C.; Tobias, G.; Duarte, I.; Vicente, R.; Marques, P.A.A.P. Bacterial Cellulose/Graphene Oxide Aerogels with Enhanced Dimensional and Thermal Stability. *Carbohydr Polym* **2020**, *230*, 115598, doi:https://doi.org/10.1016/j.carbpol.2019.115598.
28. Sandoval, S.; Kumar, N.; Sundaresan, A.; Rao, C.N.R.; Fuertes, A.; Tobias, G. Enhanced Thermal Oxidation Stability of Reduced Graphene Oxide by Nitrogen Doping. *Chemistry – A European Journal* **2014**, *20*, 11999–12003, doi:https://doi.org/10.1002/chem.201403833.
29. Gaidukevic, J.; Aukstakojyte, R.; Kozłowski, M.; Barkauskas, J.; Pauliukaite, R. A Simple Preparation of N-Doped Reduced Graphene Oxide as an Electrode Material for the Detection of Hydrogen Peroxide and Glucose. *Electrochim Acta* **2023**, *446*, 142113, doi:https://doi.org/10.1016/j.electacta.2023.142113.
30. Min, S.; Hyeon, D.S.; Jang, G.; Choi, J.; Seo, J.; Kwon, S.; Kim, D.-W.; Hong, J.P. Oxynitride Amorphous Carbon Layer for Electrically and Thermally Robust Bipolar Resistive Switching. *Adv Electron Mater* **2023**, *9*, 2201090, doi:https://doi.org/10.1002/aelm.202201090.

31. Pang, L.S.K.; Saxby, J.D.; Chatfield, S.P. Thermogravimetric Analysis of Carbon Nanotubes and Nanoparticles. *J Phys Chem* **1993**, *97*, 6941–6942, doi:10.1021/j100129a001.
32. Farivar, F.; Lay Yap, P.; Karunagaran, R.U.; Losic, D. Thermogravimetric Analysis (TGA) of Graphene Materials: Effect of Particle Size of Graphene, Graphene Oxide and Graphite on Thermal Parameters. *C (Basel)* 2021, *7*.
33. Bannov, A.G.; Popov, M. V; Kurmashov, P.B. Thermal Analysis of Carbon Nanomaterials: Advantages and Problems of Interpretation. *J Therm Anal Calorim* **2020**, *142*, 349–370, doi:10.1007/s10973-020-09647-2.
34. Sandoval, S.; Kumar, N.; Oro-Solé, J.; Sundaresan, A.; Rao, C.N.R.; Fuertes, A.; Tobias, G. Tuning the Nature of Nitrogen Atoms in N-Containing Reduced Graphene Oxide. *Carbon N Y* **2016**, *96*, 594–602, doi:https://doi.org/10.1016/j.carbon.2015.09.085.
35. Sandoval, S.; Fuertes, A.; Tobias, G. Solvent-Free Functionalisation of Graphene Oxide with Amide and Amine Groups at Room Temperature. *Chemical Communications* **2019**, *55*, 12196–12199, doi:10.1039/C9CC05693A.
36. Romanos, G.E.; Likodimos, V.; Marques, R.R.N.; Steriotis, T.A.; Papageorgiou, S.K.; Faria, J.L.; Figueiredo, J.L.; Silva, A.M.T.; Falaras, P. Controlling and Quantifying Oxygen Functionalities on Hydrothermally and Thermally Treated Single-Wall Carbon Nanotubes. *The Journal of Physical Chemistry C* **2011**, *115*, 8534–8546, doi:10.1021/jp200464d.
37. Syrgiannis, Z.; La Parola, V.; Hadad, C.; Lucío, M.; Vázquez, E.; Giacalone, F.; Prato, M. An Atom-Economical Approach to Functionalized Single-Walled Carbon Nanotubes: Reaction with Disulfides. *Angewandte Chemie International Edition* **2013**, *52*, 6480–6483, doi:https://doi.org/10.1002/anie.201301617.
38. Al-Mayman, S.I.; Al-Abbadi, N.M.; Atieh, M.A. Thermal Oxidation Kinetic of Carbon Nanotubes (CNTs). *Arab J Sci Eng* **2014**, *39*, 621–630, doi:10.1007/s13369-013-0689-8.
39. Tobón, J.I.; Paya, J.; Borrachero, M. V; Soriano, L.; Restrepo, O.J. Determination of the Optimum Parameters in the High Resolution Thermogravimetric Analysis (HRTG) for Cementitious Materials. *J Therm Anal Calorim* **2012**, *107*, 233–239, doi:10.1007/s10973-010-0997-0.
40. Archer, P.D.; Ming, D.W.; Sutter, B. The Effects of Instrument Parameters and Sample Properties on Thermal Decomposition: Interpreting Thermal Analysis Data from Mars. *Planet Sci* **2013**, *2*, 2, doi:10.1186/2191-2521-2-2.
41. Tobias, G.; Shao, L.; Salzmann, C.G.; Huh, Y.; Green, M.L.H. Purification and Opening of Carbon Nanotubes Using Steam. *J Phys Chem B* **2006**, *110*, 22318–22322, doi:10.1021/jp0631883.
42. Shao, L.; Tobias, G.; Salzmann, C.G.; Ballesteros, B.; Hong, S.Y.; Crossley, A.; Davis, B.G.; Green, M.L.H. Removal of Amorphous Carbon for the Efficient Sidewall Functionalisation of Single-Walled Carbon Nanotubes. *Chemical Communications* **2007**, 5090–5092, doi:10.1039/B712614J.
43. Ballesteros, B.; Tobias, G.; Shao, L.; Pellicer, E.; Nogués, J.; Mendoza, E.; Green, M.L.H. Steam Purification for the Removal of Graphitic Shells Coating Catalytic Particles and the Shortening of Single-Walled Carbon Nanotubes. *Small* **2008**, *4*, 1501–1506, doi:https://doi.org/10.1002/smll.200701283.
44. Cabana, L.; Ke, X.; Kepić, D.; Oro-Solé, J.; Tobías-Rossell, E.; Van Tendeloo, G.; Tobias, G. The Role of Steam Treatment on the Structure, Purity and Length Distribution of Multi-Walled Carbon Nanotubes. *Carbon N Y* **2015**, *93*, 1059–1067, doi:https://doi.org/10.1016/j.carbon.2015.06.027.
45. Foreman, J.A.; Sauerbrunn, S. Exploring the Sensitivity of Thermal Analysis Techniques to the Glass Transition.; 1997.
46. Zhai, X.; Ge, H.; Shu, C.-M.; Obracaj, D.; Wang, K.; Laiwang, B. Effect of the Heating Rate on the Spontaneous Combustion Characteristics and Exothermic Phenomena of Weakly Caking Coal at the Low-Temperature Oxidation Stage. *Fuel* **2020**, *268*, 117327, doi:https://doi.org/10.1016/j.fuel.2020.117327.
47. Cabana, L.; Ke, X.; Kepić, D.; Oro-Solé, J.; Tobías-Rossell, E.; Van Tendeloo, G.; Tobias, G. The Role of Steam Treatment on the Structure, Purity and Length Distribution of Multi-Walled Carbon Nanotubes. *Carbon N Y* **2015**, *93*, 1059–1067, doi:https://doi.org/10.1016/j.carbon.2015.06.027.
48. Garbuz, V. V; Kuzmenko, L.N.; Petrova, V.A.; Silinska, T.A.; Terentieva, T.M. Thermal Oxidation Kinetics of Multi-Walled Carbon Nanotubes in an Oxygen Flow. *Powder Metallurgy and Metal Ceramics* **2019**, *58*, 149–154, doi:10.1007/s11106-019-00058-z.
49. Ballesteros, B.; Tobias, G.; Shao, L.; Pellicer, E.; Nogués, J.; Mendoza, E.; Green, M.L.H. Steam Purification for the Removal of Graphitic Shells Coating Catalytic Particles and the Shortening of Single-Walled Carbon Nanotubes. *Small* **2008**, *4*, 1501–1506, doi:https://doi.org/10.1002/smll.200701283.

 doi:10.20944/preprints202406.0317.v1

50. Gadhavi, P.M.; Poopanya, P.; Talati, M. Structural, Electronic, and Transport Properties of Ge Doped Graphene: A DFT Study. *Physica B Condens Matter* **2023**, *666*, 415085, doi:https://doi.org/10.1016/j.physb.2023.415085.
51. Sandoval, S.; Tobias, G. Tuning the Nature of N-Based Groups From N-Containing Reduced Graphene Oxide: Enhanced Thermal Stability Using Post-Synthesis Treatments. *Nanomaterials* **2020**, *10*, doi:10.3390/nano10081451.
52. Sandoval, S.; Muthuswamy, E.; Chen, J.; Fuertes, A.; Tobias, G.; Navrotsky, A. Thermochemistry of Nitrogen-Doped Reduced Graphene Oxides. *J Eur Ceram Soc* **2020**, *40*, 6322–6327, doi:https://doi.org/10.1016/j.jeurceramsoc.2020.01.043.
53. Sandoval, S.; Kumar, N.; Sundaresan, A.; Rao, C.N.R.; Fuertes, A.; Tobias, G. Enhanced Thermal Oxidation Stability of Reduced Graphene Oxide by Nitrogen Doping. *Chemistry – A European Journal* **2014**, *20*, 11999–12003, doi:https://doi.org/10.1002/chem.201403833.